Development 125, 1137-1148 (1998)
Printed in Great Britain © The Company of Biologists Limited 1998
DEV2239

Analysis of the genetic pathway leading to formation of ectopic apical ectodermal ridges in mouse *Engrailed-1* mutant limbs

Cynthia A. Loomis*[,1,2,†], Robin A. Kimmel*[,2,3], Chun-Xiang Tong[1], Jacques Michaud[4] and Alexandra L. Joyner[2,3,5]

[1]Ronald O. Perelman Department of Dermatology, NYU Medical School, 550 First Avenue, New York, NY 10016, USA
[2]Department of Cell Biology, NYUMC, 550 First Avenue, New York, NY 10016, USA
[3]Howard Hughes Medical Institute and Developmental Genetics Program, Skirball Institute of Biomolecular Medicine, NYUMC, 540 First Avenue, New York, NY 10016, USA
[4]Department of Embryology, Carnegie Institute of Washington, Baltimore, MD 21210, USA
[5]Department of Physiology and Neuroscience, NYUMC, First Avenue, New York, NY 10016, USA
*These authors contributed equally to the work
†Author for correspondence (email: loomic01@mcrcr.med.nyu.edu)

Accepted 24 December 1997: published on WWW 17 February 1998

SUMMARY

The apical ectodermal ridge (AER), a rim of thickened ectodermal cells at the interface between the dorsal and ventral domains of the limb bud, is required for limb outgrowth and patterning. We have previously shown that the limbs of *En1* mutant mice display dorsal-ventral and proximal-distal abnormalities, the latter being reflected in the appearance of a broadened AER and formation of ectopic ventral digits. A detailed genetic analysis of wild-type, *En1* and *Wnt7a* mutant limb buds during AER development has delineated a role for *En1* in normal AER formation. Our studies support previous suggestions that AER maturation involves the compression of an early broad ventral domain of limb ectoderm into a narrow rim at the tip and further show that *En1* plays a critical role in the compaction phase. Loss of *En1* leads to a delay in the distal shift and stratification of cells in the ventral half of the AER. At later stages, this often leads to development of a secondary ventral AER, which can promote formation of an ectopic digit. The second AER forms at the juxtaposition of the ventral border of the broadened mutant AER and the distal border of an ectopic *Lmx1b* expression domain. Analysis of *En1/Wnt7a* double mutants demonstrates that the dorsalizing gene *Wnt7a* is required for the formation of the ectopic AERs in *En1* mutants and for ectopic expression of *Lmx1b* in the ventral mesenchyme. We suggest a model whereby, in *En1* mutants, ectopic ventral *Wnt7a* and/or *Lmx1b* expression leads to the transformation of ventral cells in the broadened AER to a more dorsal phenotype. This leads to induction of a second zone of compaction ventrally, which in some cases goes on to form an autonomous secondary AER.

Key words: Limb development, *Engrailed-1*, AER, Mouse, *Wnt7a*, *Lmx1b*

INTRODUCTION

Classical tissue transplantation experiments and recent genetic studies in the limb indicate that 'signalling centers' provide the molecular cues necessary for patterning the limb and directing regional outgrowth along the three different axes (Saunders, 1948 and/or Martin, 1995; Johnson et al., 1994; Tickle, 1995; Niswander, 1996; Zeller and Duboule, 1997). One such signalling center is the apical ectodermal ridge (AER), a narrow rim of thickened ectoderm along the limb margin. The AER is critical for normal proximal-distal limb outgrowth (Saunders, 1948) and this function appears to be mediated by members of the fibroblast growth factor family, such as Fgf4 and Fgf8 (Niswander et al., 1993; Ohuchi et al., 1995; Mahmood et al., 1995; Crossley et al., 1996; Vogel et al., 1996). Patterning along the anterior-posterior (A-P) axis is specified by the zone of polarizing activity (ZPA), a cluster of mesenchymal cells in the posterior limb bud (Saunders and Gasseling, 1968). A major component of the ZPA signalling cascade is the protein Sonic hedgehog (Shh) (Riddle et al., 1993). Dorsal-ventral (D-V) axis polarity is influenced by the non-AER ectoderm (Pautou and Kieny, 1973; MacCabe et al., 1974; Pautau, 1977; Geduspan and MacCabe, 1987, 1989; Akita, 1996). Wnt7a, a secreted factor expressed by the dorsal limb ectoderm, is required for the differentiation of dorsal mesenchymal structures (Parr et al., 1993; Parr and McMahon, 1995) and mis-expression studies in chick suggest it acts by inducing expression of the LIM homeodomain-containing gene, *Lmx1b*, in the underlying mesenchyme (Riddle et al., 1995; Vogel et al., 1995). Engrailed-1 (En1), a homeodomain-containing transcriptional regulator expressed in the ventral limb ectoderm (Davis et al., 1991; Gardner and Barald, 1992), is critical for directing the development of ventral limb structures and appears to act in part by suppressing *Wnt7a*

function in the ventral limb (Loomis et al., 1996; Logan et al., 1997). Recent studies have shown that the function of these different signalling regions is interdependent. Shh signalling by the ZPA is required for maintenance of the AER (Laufer et al., 1994; Niswander et al., 1994), and *Fgf4* and *Wnt7a* expression are required for maintenance of Shh expression ((Laufer et al., 1994; Niswander et al., 1994; Parr and McMahon, 1995; Yang and Niswander, 1995).

Our studies of mice homozygous for *En1* loss-of-function alleles suggested that an additional regulatory relationship exists between D-V limb patterning genes and AER formation. *En1* mutant limbs not only demonstrate a partial dorsal transformation of the ventral paw, but they also display a ventroproximal expansion of the AER (Loomis et al., 1996). We suggested that this expansion of the newly formed AER could be responsible for the presence of ectopic ventral digits on the proximal paws of some mutants. In keeping with our findings, recent misexpression studies in chick have shown that ectopic expression of *En1* in the AER and dorsal chick limb either ablates normal AER development or results in ectopic secondary AERs (Laufer et al., 1997; Logan et al., 1997; Rodriguez-Esteban et al., 1997). Recent mutant and misexpression experiments in chick (Laufer et al., 1997; Rodriguez-Esteban et al., 1997), as well as mutant studies in mouse (Sidow et al., 1997), indicate that Notch signaling also plays a role in AER development. One of the molecules in this pathway, R-fng, has been shown to be dorsally restricted in chick limbs and appears to be regulated in part by *En1* (Laufer et al., 1997; Rodriguez-Esteban et al., 1997).

Correlative molecular data in several chick mutants also suggest a link between D-V patterning and AER development. In the chick *limbless* mutant in which limb outgrowth does not occur due to failure to form an AER (Prahlad et al., 1979), molecular studies demonstrate that expression of AER marker genes is not initiated and normal D-V axis asymmetries are not established (Grieshammer et al., 1996; Noramly et al., 1996; Ros et al., 1996). Expression of *Wnt7a* and *Lmx1b* is expanded into the ventral limb, whereas expression of the ventralizing gene, *En1*, is absent in these mutants. On the contrary, chick *wingless* mutant limb buds initiate *Fgf8* expression and display proper D-V patterning early on, but they subsequently fail to form a differentiated AER and molecular D-V asymmetries are lost (Ohuchi et al., 1997).

Based on experimental studies of *Drosophila* limb development and theoretical considerations in mouse, Meinhardt suggested that the juxtaposition of dorsal and ventral limb domains might be a precondition for normal vertebrate AER development (Meinhardt, 1983). In addition to the studies outlined above, further support for Meinhardt's hypothesis is provided by recent grafting experiments in avian limbs. Chimera studies in which presumptive dorsal or ventral quail limb tissue was inserted into ventral or dorsal limb domains, respectively, resulted in formation of ectopic AERs along the borders between chick and quail tissues (Tanaka et al., 1997). Moreover, the replacement of dorsal chick ectoderm with ventral chick ectoderm at slightly later stages of limb bud development also led to the formation of ectopic AERs (Laufer et al., 1997).

In an effort to better understand the potential relationship between D-V patterning and AER formation, we have used morphological criteria as well as expression analysis of several genetic markers to compare early AER development and subsequent maturation in wild type as well as *En1*, *Wnt7a* and *En1/Wnt7a* double-mutant mice. Our results indicate that early mesenchymal D-V patterning is normal in *En1* mutant mice whereas ventral ectoderm specification in *En1* mutants is abnormal even at early stages of limb development. At later stages, mesenchymal patterning is abnormal as *Lmx1b* is reexpressed in the ventral mesenchyme. Moreover, maturation of the AER is aberrant resulting in an expanded ventral AER. With further development, a bifurcated AER is formed following stratification of the ventral border of the mutant AER. Interestingly, ectopic ectodermal stratification occurs at the distal edge of the ventral *Lmx1b* expression domain. In some cases, the (anatomically) ventral AER rim goes on to form a secondary AER capable of promoting ectopic digit development. Finally, analysis of *Wnt7a/En1* double mutants demonstrates that *Wnt7a* is required for both the ectopic ventral expression of *Lmx1b* and the development of ectopic secondary AERs and ventral digits in *En1* mutant limbs.

MATERIALS AND METHODS

Genotype analysis of *En1*, *Wnt7a* and *En1/Wnt7a* mutant mice

The *En1* and *Wnt7a* mutants used in these studies were previously generated by targeted disruption of the respective genes (Wurst et al., 1994; Hanks et al., 1995; Parr and McMahon, 1995; Matise and Joyner, 1997). In the case of the $En1^{lki}$ allele, the bacterial *lacZ* coding sequences were targeted to the *En1* locus, bringing them under the control of the *En1* regulatory sequences and inactivating En1 protein function (Hanks et al., 1995; Matise and Joyner, 1997). *En1/Wnt7a* double mutants were generated by crossing mice heterozygous for both alleles since homozygosity results in perinatal lethality and/or sterility. DNA was isolated from either yolk sacs or tails and genotyping was performed by either Southern blot analysis as previously described (Hanks et al., 1995) or PCR analysis. Primers used for genotyping the *En1* wild-type allele were 5′-GTTCCAGGCAAACCGCTATATC-3′ and for the $En1^{hd}$ allele were 5′-GCCAGCTCATTCCTCCCACTC-3′ and 5′-CGGTCGTAAGCAGTTTGGCATG-3′. Primers used to genotype the *Wnt7a* wild-type allele were 5′-CTCTTCGGTGGTAGCTCTGG-3′ and 5′-CCTTCCCGAAGACAGTACGC-3′ and for the *Wnt7a* null allele were 5′-TCACGTCCTGCACGACGCGAGCTG-3′ and 5′-CCTTCCCGAAGACAGTACGC-3′ (Cygan et al, 1997).

Histology and in situ hybridizations

Digoxigenin-labelled whole-mount and ^{35}S-labelled section RNA in situ hybridizations were performed essentially as described (Loomis et al., 1996; Matise and Joyner, 1997). The probes used were to *En1* (Wurst et al., 1994), *Wnt7a* (Parr and McMahon, 1995), *Fgf8* (Crossley and Martin, 1995), *Fgf4* (Niswander and Martin, 1992), *Dlx2* (Robinson and Mahon, 1994), *Jag1* (Lindsell et al., 1995) and *Lmx1b* (Cygan et al., 1997). *Lmx1b* is the mouse homolog of the previously characterized chick *Lmx1* gene (Cygan et al., 1997). Embryos for β-galactosidase staining were fixed for 20 minutes to 1 hour, depending on the age, in 4% paraformaldehyde in phosphate-buffered saline on ice and then stained with either X-gal (Sigma) or salmon-gal (Biosynth) substrates diluted in a standard staining buffer containing both 0.02% NP-40 and 0.01% deoxycholate and incubated overnight at room temperature. Some salmon-gal stained embryos were used for double labelling by RNA in situ hybridization. These embryos were postfixed for 24 hours in 4% paraformaldehyde at 4°C and then hybridized with RNA probes as above, omitting the bleaching and methanol dehydration steps

(Matise and Joyner, 1997). Proteinase K treatments were also reduced so that embryos were incubated in either 2 μg/ml or 0.5 μg/ml for 5 minutes at 37°C for probes to mesenchymal or ectodermal mRNAs, respectively. Cryosections of embryos used in whole-mount RNA in situ hybridizations were prepared by first sinking the embryos in 15% sucrose overnight followed by 30% sucrose for 4 hours. The embryos were then embedded in OCT medium and cut at 10-40 μm.

RESULTS

D-V and AER marker gene expression in early pre-AER limb buds

Our previous analysis of the *En1* mutant AER defect focused on the limb bud stage when a definitive, multilayered AER arises in wild-type mice (10.5 dpc for the forelimb and 11.5 dpc for the hindlimb). To begin to understand the genetic events that trigger and sustain the development of an aberrant AER in *En1* mutants, we performed a detailed analysis of the expression patterns of AER and D-V marker genes in wild-type and mutant limb buds. For consistency, we adopted the mouse limb staging system first developed by Wanek et al. (1989) and modified by Bell and Scott (personal communication). At stage 0.25, the limb bud is not yet morphologically discernable along the embryo flank but, by stage 0.5, it is delineated by a slight prominence and its ventral ectoderm is slightly thickened compared to the flattened dorsal ectoderm. At stage 1, the limb is a broad bulge with the distoventral ectoderm thickened relative to the dorsal and more proximal ventral ectoderm (see Fig. 1B,E,H,K). At stage 2, the limb bud looks like a semicircular protrusion emanating from the flank, and a broad crescent or band of bilayered ectoderm is present on the distal third of the ventral limb (Milaire, 1974). At stage 3 (10.5 dpc in the forelimb), the definitive, mature AER is visible along the distal rim of the elongated, cylindrical limb bud and consists of 3-4 layers of ectodermal cells (see Fig. 1C,F,I,L). In mouse, the AER appears to form a true stratified epithelium (Kelley and Fallon, 1983).

Molecular analysis of wild-type limb buds prior to the formation of a morphologically distinct AER demonstrated dynamic shifts in the topological location of both D-V and AER marker gene expression domains. Between stages 0.25 and 0.5, the AER marker gene *Dlx2* was expressed throughout the ventral ectoderm (data not shown) but, by stage 1, the *Fgf8/Dlx2* expression domain occupied only the distal half of the ventral limb bud (Fig. 1D,E). Over the next few stages, this domain was compressed even further so that *Dlx2* and *Fgf8* expression was ultimately restricted to the multilayered AER along the D-V interface (Fig. 1F). Over the same stages, the *En1* expression domain shifted distally, from a relatively restricted proximoventral position to extend over the entire ventral limb including the ventral AER (Fig. 1A-C). In parallel with these relative distal shifts in the topological location of AER and ventral ectoderm marker genes, the 'dorsal' marker genes, *Wnt7a* and *Lmx1*, were also displaced more dorsally (Fig. 1G-L). *Wnt7a*, which at stage 1 was expressed in the distal and dorsal ectoderm covering 2/3 of the limb, became restricted to only the dorsal half of the limb ectoderm by stage 3 (Fig. 1H,I). *Lmx1b*, which was found to be expressed in both the ventral and dorsal limb mesenchyme prior to stage 2, became restricted to the dorsal mesenchyme by stage 3 (Fig. 1K,L).

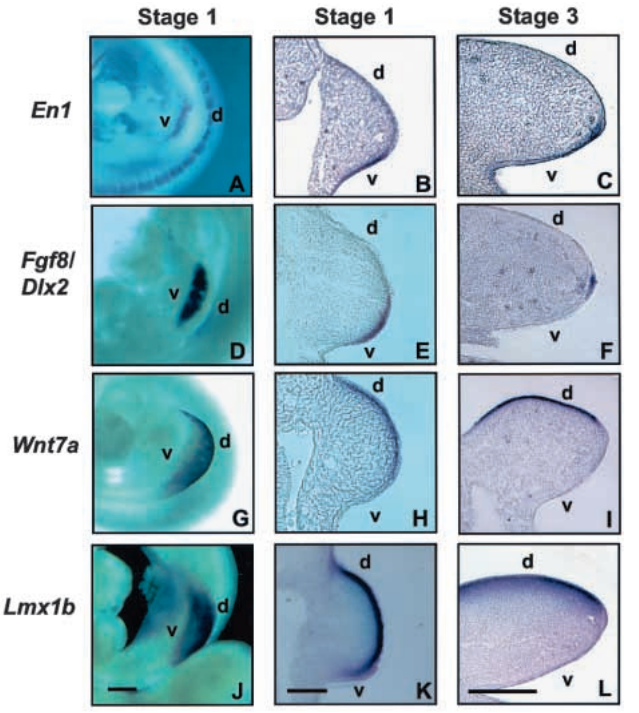

Fig. 1. The position of D-V and AER marker gene expression shifts dorsodistally during the transition from a pre-AER to an AER stage limb bud. Whole-mount RNA in situ hybridization and subsequent sagittal cryosections of wild-type limbs at stage 1 (A,B,D,E,G,H,J,K) and stage 3 (C,F,I,L). Dorsal (d) and ventral (v) as indicated. (A-C) *En1* expression in the early limb bud. Note the distal shift of *En1* expression from a proximoventral position at stage 1 (A) to a broad region encompassing both the ventral ectoderm and ventral AER at stage 3 (B,C). (D,F) *Fgf8* and (E) *Dlx2* expression was detected in a broad domain of thickened ectoderm along the distal half of the ventral limb bud at stage 1 (D,E), but by stage 3 this expression domain had both compressed and shifted distally, delineating the definitive AER (F). Note that the position of morphologically thickened ectoderm shifted in parallel with AER marker gene expression. (G-I) Early *Wnt7a* expression was detected throughout much of the dorsal and ventral limb ectoderm but, by stage 3, had become restricted to the dorsal surface. *Lmx1b* expression (J-L) was initially in a broad region that included ventral, distal and dorsal mesenchyme but, by stage 3, had became restricted to the dorsal mesenchyme. Mesenchymal staining is limited to a superficial band due to incomplete penetration of the probe. Bar: 100 μm.

Differentiation and compression of the ventral AER are aberrant in *En1* mutant embryos

To determine if *En1* plays a role in setting up the expression domains in the early limb bud, we conducted the same analysis in *En1* mutant embryos. D-V ectodermal patterning was abnormal even at the earliest limb stages. Ectopic ventral expression of *Wnt7a* could be detected as early as stage 0.5 in *En1* mutants (data not shown), with intense expression persisting in the ventroproximal ectoderm but clearing from the ventrodistal ectoderm of older pre-AER and AER stage limbs (Fig. 2 compare A and B, E and F). In contrast, expression of

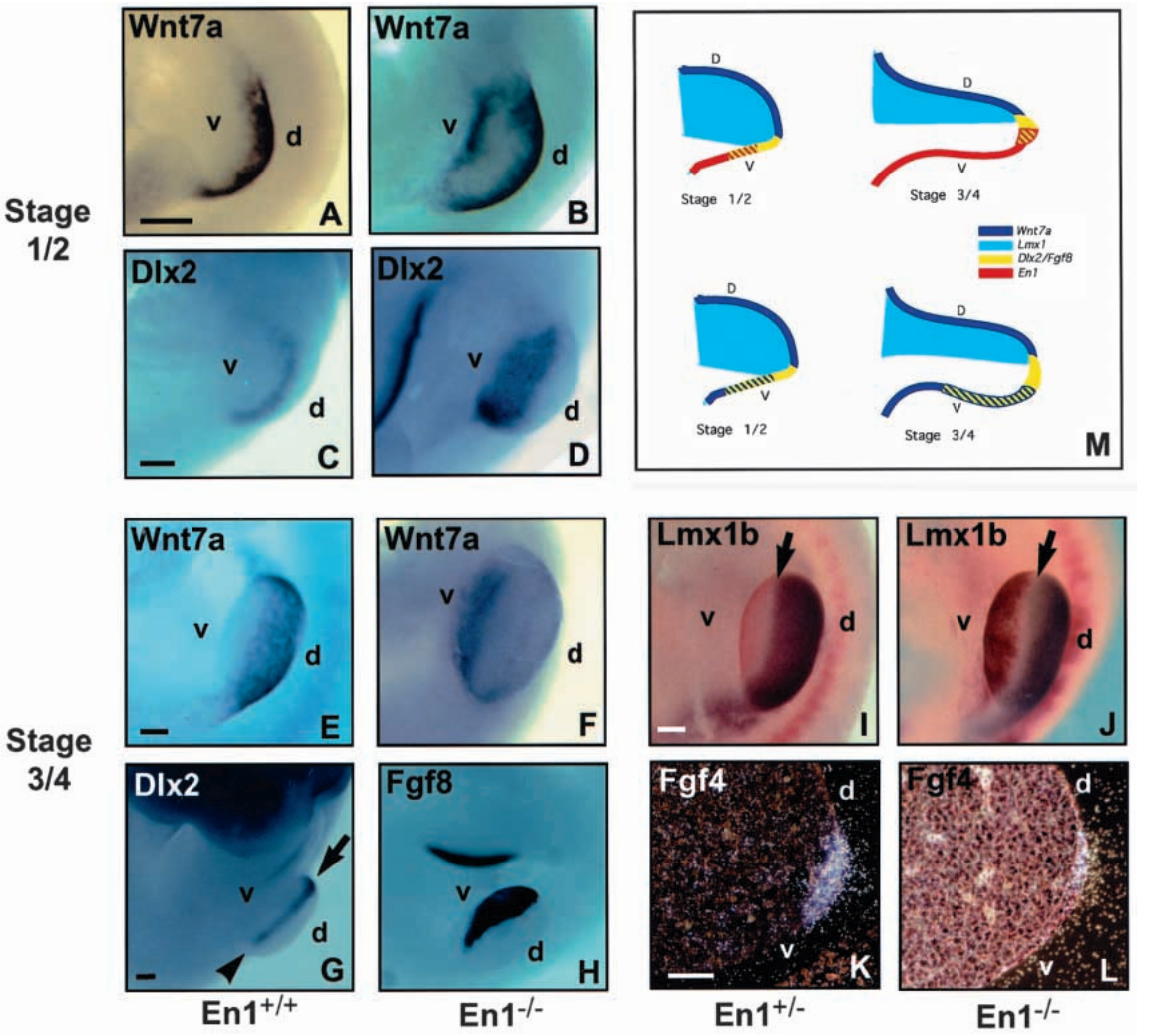

Fig. 2. Ectodermal D-V patterning and early AER differentiation is abnormal in *En1* mutant limbs. (A-J) Whole-mount and (K,L) section RNA in situ hybridizations of limbs from wild-type or *En1* heterozygous mice (A,C,E,G,I,K) and *En1* mutant mice (B,D,F,H,J,L) at stages 1/2 (A-D) and 3/4 (E-L). Dorsal (d) and ventral (v) as indicated. (A,B,E,F) *Wnt7a* probe illustrating the ectopic ventral expression in mutant limb buds (B,F) compared to wild-type limbs (A,E). Note the central clearing of *Wnt7a* expression from the ventrodistal ectoderm in the mutant limb buds (B,F). (C,D,G) *Dlx2* and (H) *Fgf8* probes demonstrating the marked ventroproximal expansion of the expression domain in mutant embryos (D,H), compared to wild-type embryos (C,G). Note that at stage 3, the AER, as delineated by *Dlx2* expression, is slightly broader anteriorly (arrow) than posteriorly (arrowhead). (I,J) Double-label whole mounts for *En1-lacZ* expression (pink) and *Lmx1b* expression (purple) demonstrating that cells expressing *En1-lacZ* are present throughout the ventral limb ectoderm, extending to the distal tip, and that *Lmx1b* expression is dorsally restricted in stage 3 limbs from *En1* heterozygotes (I) and mutants (J). Note the clear distal area devoid of probe which demarcates the location of the dorsal AER. The greater intensity of β-galactosidase staining in mutant compared to heterozygous limbs is due in part to the presence of two *lacZ*-targeted *En1* alleles. Section in situ hybridization of stage 3/4 (K) wild-type and (L) *En1* mutant limbs using a ^{35}S-labelled *Fgf4* probe. Note the restriction of *Fgf4* expression to the dorsal-most portion of the partially stratified mutant AER (L) compared to its expression throughout the dorsal and ventral halves of the wild-type AER (K). (M) Schematic illustrating the expression pattern of these genes in stage 1/2 and stage 3/4 limb buds. Bar: 100 μm.

the mesenchymal gene *Lmx1b* was normal in *En1* mutant limbs at these early stages as it was appropriately expressed in early dorsal and ventral mesenchyme and then repressed despite persistent expression of *Wnt7a* in the adjacent ventral ectoderm (Fig. 2I,J and data not shown).

AER marker gene expression was initiated normally in *En1* mutant limb buds, but failed to shift distally as occurs in wild-type limb buds. The *Fgf8/Dlx2* expression domain in stage 1 *En1* mutant limbs was clearly broader than in wild-type limbs (Fig. 2, compare C and D). By stage 3/4, although the proximal boundary of the *Dlx2/Fgf8*-positive domain had shifted distally slightly, the mutant AER remained much broader than its wild-type counterpart (Fig 2, compare G and H). Expression of *Fgf4*, a late stage AER differentiation marker, was mainly restricted to the dorsal-most cells of the *En1* mutant AER (Fig. 2K,L).

To determine whether the expanded portion of the *En1* mutant AER corresponded primarily to the ventral AER, which normally expresses *En1*, we analyzed mice heterozygous or homozygous for an *En1* targeted null allele, *En1*^{lki} (Hanks et al., 1995; Matise and Joyner, 1997), which expresses the *lacZ*

reporter gene from the *En1* locus. Double labelling for β-galactosidase activity (*En1-lacZ* expression) and *Lmx1b* mRNA showed that, by stage 3 in both $En1^{lki/+}$ and $En1^{lki/lki}$ mutants, the size of the dorsal AER, delineated as the 'negative' domain between *Lmx1b* expression dorsally and *lacZ* ventrally, was very similar (Fig. 2I,J). These observations, together with the *Fgf4* expression data and our previous molecular and morphological studies (Loomis et al., 1996), indicate that the dorsal AER is not grossly altered in *En1* homozygous mutants; *En1* appears to be required primarily for compaction and maturation of the ventral AER.

Development of a second ectodermal thickening along the proximoventral boundary of the expanded *En1* mutant AER

Since the ventroproximally expanded AER detected in *En1* mutant forelimb buds at stage 3 (Loomis et al., 1996) resembled the thickened ectoderm normally seen in a stage 2 wild-type limb, one question was whether the ventral expansion of the *En1* mutant AER at 10.5 dpc simply reflected a delay in the distal shift of cells expressing *Dlx2/Fgf8*. To address this, we compared AER morphology and marker gene expression patterns in wild-type and mutant limbs at later stages of maturation and found that, over the next several stages, the *En1* mutant AER expression domain remained broader than the wild-type AER expression domain (compare Fig. 3A,C with B,D). Surprisingly, whole-mount gene expression analyses revealed that, at limb stages 5/6, the ventral expansion of the *En1* mutant AERs exhibited a marked A-P asymmetry (Fig. 3B), which was not prominent at limb stages 3/4 (Fig 2D). The anterior half of the *En1* mutant AER at these stages was up to 4-6 times wider than the normal AER, whereas the posterior half was usually only 2-3 times wider than the wild type. This A-P asymmetry was observed in 90% of limbs analyzed (n>40) using a variety of AER-specific probes.

In addition to its marked anterior expansion, the *En1* mutant AER also appeared to bifurcate into two distinct ectodermal ridges between stages 5 and 7. In situ staining with *Fgf8* or *Dlx2* riboprobes outlined two intensely stained rims of ectoderm, which were separated by an intervening region of less intensely stained epithelium (Fig. 3B). The dorsal rim was anchored at the distal limb margin whereas the ventral rim formed along the ventroproximal boundary of the expanded *Dlx2/Fgf8* expression domain.

Roughly coincident with the formation of the second ventral AER rim, *Lmx1b* was re-expressed in the ventral mesenchyme of stage 5/6 *En1* mutant limbs (Fig. 3E,F). We were somewhat surprised that ventral *Lmx1b* reexpression was initiated at such a late developmental stage in the ventral mesenchyme given the persistent expression of *Wnt7a* in the ventral ectoderm and the reported role of *Wnt7a* in promoting *Lmx1b* expression in chick (Riddle et al., 1995; Vogel et al., 1995). To more directly assess the regulatory relationship of these two genes in mouse, we analyzed *Lmx1b* expression in *Wnt7a* mutant mice. We found that *Lmx1b* expression was initially normal but, beginning at stages 5/6, expression was markedly decreased in the distodorsal mesenchyme adjacent to the ridge (Fig. 3I). Thus, in mouse, *Wnt7a* appears to regulate *Lmx1b* expression only at later stages of development.

Despite the intense reexpression of *Lmx1b* in the ventroproximal mesenchyme of *En1* mutant mice, the mesenchyme directly beneath the mutant AER did not reexpress *Lmx1b*. The striking A-P asymmetry of the AER was

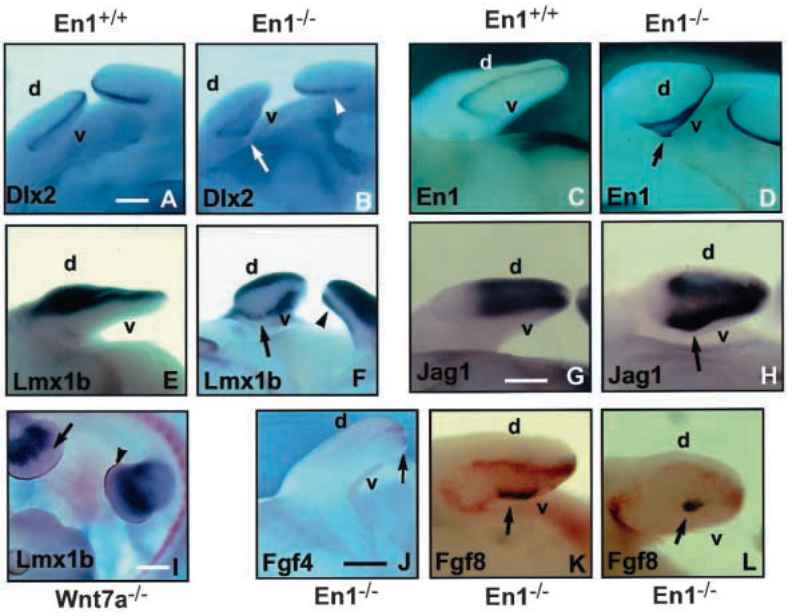

Fig. 3. Loss of *En1* function results in reexpression of *Lmx1b* ventrally and abnormal AER maturation, leading in some cases to formation of ectopic AERs. Whole-mount in situ hybridization and/or β-galactosidase staining of stage 5/6 (A-H,J) and stage 7/8 (I,K,L) wild-type (A,C,E,G), *En1* mutant (B,D,F,H,J-L) and *Wnt7a* mutant limbs (I). Dorsal (d) and ventral (v) are indicated. *Dlx2* probe (A,B) illustrating the intense staining of the dorsal and ventral rims of the bifurcated mutant AER and the marked widening anteriorly (arrow, B) relative to posteriorly (arrowhead, B) and compared to the narrow ridge of a wild-type AER (A). β-galactosidase staining (C,D) demonstrating the strong expression of *En1-lacZ* in the AER and weaker staining in the ventral ectoderm of limbs from (C) heterozygous and (D) homozygous mice. Again note the mutant AER is wider anteriorly (arrow) versus posteriorly (arrowhead). *Lmx1b* probe (E,F) illustrating the normal dorsal expression (E) and the ectopic reexpression in the ventral mesenchyme of *En1* mutant limbs (F). Note that the contours of the distal *Lmx1b*-negative zone have the same contours of an expanded AER. *Jagged-1* expression (G,H), which was restricted to the progress zone of wild-type limb buds (G), extended into these ventral mesenchymal bulges associated with the marked anterior widening of the *En1* mutant AERs (H, arrow). *Lmx1b* expression (purple) in a stage 5/6 *Wnt7a* mutant hindlimb (I, arrowhead) is relatively normal and nearly abuts the *En1-lacZ* marked AER (pink). However, a distal *Lmx1b*-negative zone is clearly present in the more mature, stage 7/8 forelimb (I, arrow). *Fgf4* expression (J) in the dorsal rim and a small region of the ventral rim of the bifurcated En1 mutant AER (arrow). *Fgf8* expression (purple,K,L) reveals persistent focal expression (arrows) in the ventral ectoderm of some *En1* mutant limbs at about the time when *Fgf8* transcripts are down-regulated in the primary AER, which is delineated by intense *En1-lacZ* expression (pink). These secondary AER signalling centers always overlie ectopic mesenchymal outgrowths. Bar: 500 μm.

paralleled by a marked A-P asymmetry in the breadth of the *Lmx1b*-negative mesenchymal zone. Thus, the 'footprint' of the widened mutant AER overlaid the Lmx1b-negative zone and appeared to be outlined by the dorsal and ventral *Lmx1b* expression boundaries.

Development of autonomous secondary AERs in *En1* mutant limbs

The AER is a transitory embryonic structure and, by stages 6-8, most AER-specific genes, including *Fgf4* and *Fgf8*, are down-regulated and the AER begins to flatten and regress (Jurand, 1965; Milaire, 1974; Wanek et al., 1989). In some stage 6-8 *En1* mutant limbs, however, clusters of cells associated with the ventral AER rim continued to express AER marker genes when they were fading elsewhere (Fig. 3J-L). These ectopic signalling centers were always associated with underlying mesenchymal outgrowths. As would be predicted if the signalling centers function as AERs, such mesenchymal bulges expressed genes normally restricted to cells of the progress zone that underlie the AERs, such as *Evx1* (Niswander and Martin, 1993) and *Jagged-1* (Fig. 3G,H and data not shown). *Shh*, a component of the pathway directing A-P patterning of the distal limb, was rarely detected in the ectopic outgrowths (data not shown). Although almost all *En1* mutant limbs demonstrated a marked ventral expansion of the anterior half of the bifurcated AER, only 30-40% (n>40) of mutant limbs gave rise to secondary signalling centers with persistent AER-marker expression. In addition, the formation of such signalling domains occurred only in anterior regions near the widest separation between the dorsal and ventral AER rims.

By limb stages 9-11, the normal regressing AER is difficult to distinguish morphologically from the adjacent ventral and dorsal ectoderm (Wanek et al., 1989). Interestingly, analysis of β-galactosidase activity in limbs of mice carrying the $En1^{lki}$ allele, suggested that a remnant ridge persists along the D-V boundary (Fig. 4A,B) up to at least stage 13 (16.5 dpc) in normal embryos. Relatively intense *En1* mRNA expression also delineated a D-V boundary zone up to at least stage 12 (15.5 dpc, data not shown), indicating that the persistent β-galactosidase activity did not solely reflect stability of the β-galactosidase protein.

β-galactosidase activity in $En1^{lki/lki}$ mice was used to follow the evolution of the mutant ectopic AERs. As shown in Fig. 4C, the anterior ventral rim of a stage 8/9 mutant limb was shifted more distally than what was observed at earlier developmental stages, thus positioning the ventral rim in closer proximity to the dorsal rim. In some mutant limbs at this stage (n=5/16 limbs analyzed), the dorsal and ventral rims had become very closely apposed, producing a narrow linear ridge along the D-V interface, which was only slightly wider than the wild-type counterpart (Fig. 4A,B).

In other mutant limbs (n=8/16), however, a region of the ventral ridge remained associated with proximal mesenchymal outgrowths and, as a result, formed a small deflection or bow in the otherwise linear contour of the ventral rim (Fig 4D). Over the next few developmental stages, such bows were completely replaced by linear ridges (n=3/16 at stages 8-9 and n=6/12 at stages 10-12) which intersected the primary ridge at a 90° angle (Fig. 4E,F). In some cases, a proximal segment of the ventral AER rim became discontinuous with the primary rim and was at an approximately 90° angle to the primary rim (5/30, stages 8-12). These more proximal, autonomous ridges always overlaid elongated outgrowths, which resembled developing digits (Fig 4G,H,K). Intermediate stages could

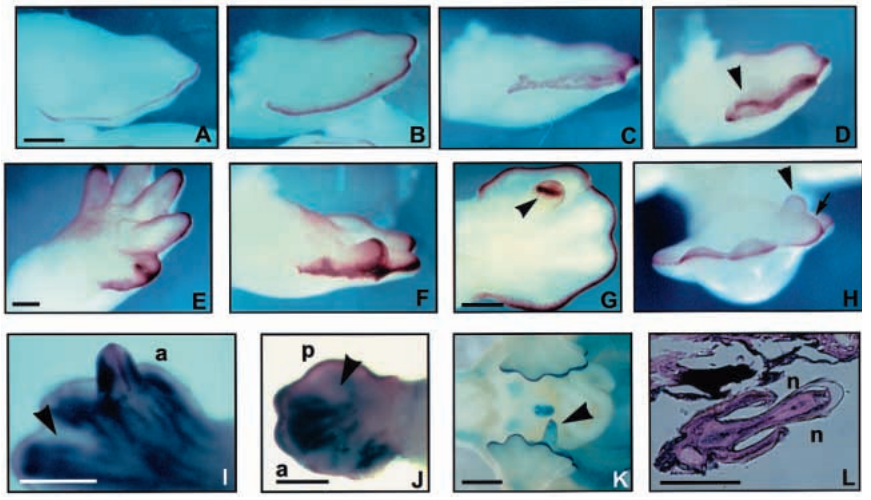

Fig. 4. Further constriction of the bifurcated ridge and reorientation of the ectopic ventral AERs. Ventral views of β-galactosidase-stained heterozygous ($En1^{lki/+}$) (A) and *En1* mutant ($En1^{lki/hd}$) (B-H) limbs between stages 9 and 12. *En-lacZ* expression outlining the narrow, phenotypically wild-type AER (A) at these later stages and the apparent distal shift of the ventral rim of the bifurcated *En1* mutant AER (B,C). In some *En1* mutant limbs at this stage, the ventral rim has become tightly apposed to the dorsal rim (B). Nevertheless, the *En1* mutant AER in B stains more intensely than the phenotypically wild-type AER (A) even though both the mutant ($En1^{lki/hd}$) and the ($En1^{lki/+}$) heterozygotes carry a single $En1^{lki}$ reporter allele. In other *En1* mutant limbs at this stage, the ventral rims are not yet tightly apposed to the dorsal rims, and at positions of focal mesenchymal outgrowths the ventral rims display a proximoventral bow or deviation in their otherwise linear course (D, arrowhead). With time all such bows are replaced by secondary linear ridges which join the AER at a 90° angle (E,F). Secondary ridges which developed more proximally overlie differentiating ectopic digits and appear to be discontinuous with the primary ridge at this stage (G, arrowhead). However, if viewed from the side, some are found to be linked to the primary AER through a residual mesenchymal thickening (H, arrow). *Lmx1b* expression (purple) illustrates the double dorsal nature of a ventral outgrowth in a stage 10 limb bud (I). *En1-lacZ* expression (pink) demarcates the position of the ectopic secondary AER. The two dorsal domains are on the anterior (a) and posterior aspects of the ectopic outgrowth and the proximal-distal axis is perpendicular to the primary P-D axis. Note the absence of *Lmx1b* staining in the interdigital region (arrowhead, I). By these later time points, *Lmx1b* expression has cleared (arrowhead, J) from the posterior (p) ventral hand plate. *En-lacZ* (blue) expression illustrating an early ventral digit in a stage 12 *En1* mutant limb (K). Hematoxylin and eosin stained sagittal sections of a well differentiated *En1* mutant ventral digit (L) demonstrating nail plates (n) on both the dorsal and ventral surfaces, confirming the double-dorsal nature of these structures. Bar: 500 μm.

occasionally be detected in which such autonomous *En1-lacZ*-positive ridges could be shown to be indirectly connected to the primary ridge through a ventral mesenchymal thickening (Fig. 4H).

Lmx1b expression boundaries are associated with ectopic secondary AERs

Lmx1b limb expression, like *En1*, persisted long after most AER-specific marker genes and *Wnt7a* expression had faded. By stage 9, *Lmx1b* expression was closely associated with the developing dorsal skeletal elements of the foot and had cleared from the interdigital webs of the dorsal domains of both wild-type and mutant limbs (Fig. 4I).

The ventral *Lmx1b* expression pattern in *En1* mutant limb buds at these later stages demonstrated several striking features. First, the pattern of interdigital web clearing of *Lmx1b* was more irregular on the ventral limb than on the dorsal limb. Second, *Lmx1b* expression was not maintained in the posterior ventral footplate (Fig. 4J). This observation was consistent with our earlier observation that the posterior-most digits of *En1* mutant limbs were less dorsalized than the more anterior digits (Loomis et al., 1996). Second, there was dramatic clearing of *Lmx1b* expression below the ectopic AERs (Fig. 4I). This was similar to the striking *Lmx1b*-negative footprint produced by the widened primary AER at earlier stages in the *En1* mutant limbs. Finally, the ectopic ventral outgrowths expressed *Lmx1b* on both sides of the *Lmx1b*-negative zone beneath the ectopic AERs, suggesting they had a double-dorsal identity (Fig. 4I). Interestingly, the two *Lmx1b*-positive dorsal domains were on the anterior and posterior sides of the ectopic digit relative to the rest of the limb, reflecting the 90° rotation of the ectopic ridge. In rare *En1* homozygotes that survive past birth, it was clear that morphologically, the well-differentiated ventral digits have cylindrical nails similar to the *En1* double-dorsal digits (Fig. 4L).

Wnt7a is required for ectopic ventral digit formation in *En1* mutants

Our expression studies implicated the ectopic expression of *Wnt7a* and *Lmx1b* in the formation of ectopic AERs and digit formation. To further investigate this association, *En1/Wnt7a* double homozygous mutants were constructed by interbreeding *En1* and *Wnt7a* heterozygotes (Wurst et al., 1994; Hanks et al., 1995; Parr and McMahon, 1995; Matise and Joyner, 1997). In *En1/Wnt7a* double mutants, as in the *Wnt7a* mutants, the AERs were found to be slightly (1.5-2 fold) wider than wild-type AERs (Fig. 5A,C,D), and staining for *En1-lacZ* expression suggested that the dorsal, rather than the ventral, portion of the AER was primarily expanded in these mutants (data not shown). None of the stage 3/4 *En1/Wnt7a* double mutant AERs (n=12) displayed the dramatic ventral expansion characteristic of *En1* mutant AERs (Fig. 5B). Also, none of the AERs of stage 5-8 *En1/Wnt7a* double mutants developed a second ventral rim or appeared bifurcated (n=16). This is in contrast to the >90% of *En1* mutant limbs which display these features. Finally, none of the stage 7-10 *En1/Wnt7a* double-mutant embryonic limbs displayed ventral mesenchymal outgrowths associated with functional ectopic AERs (n=8) nor did postnatal double mutants have ectopic ventral digits (n=30). Thus, ectopic *Wnt7a* signalling in the ventral ectoderm appears to be essential for the delay in compaction of the ventral *En1* mutant AER and for subsequent ectopic AER and digit formation.

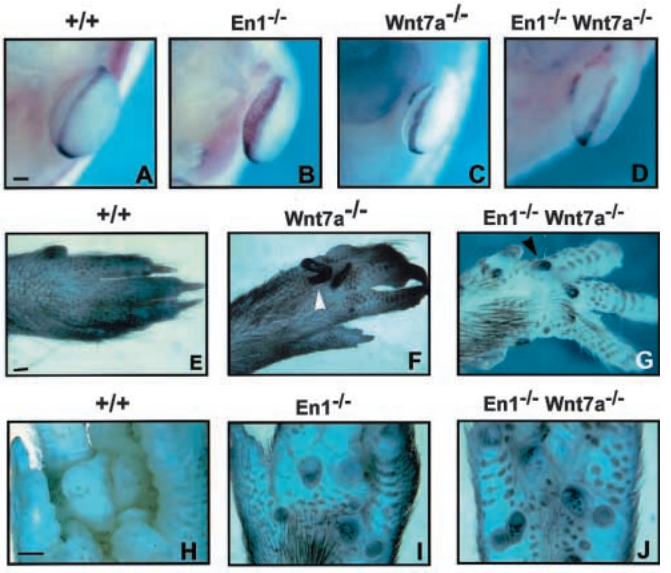

Fig. 5. Formation of an *En1* mutant AER and certain D-V patterning defects requires *Wnt7a* expression. (A-D) Whole-mount RNA in situ hybridizations of stage 4 wild-type (A), *En1* mutant (B), *Wnt7a* mutant (C) and *En1/Wnt7a* double-mutant (D) limb buds probed with *Fgf8* (purple). Some of the embryos were also stained for *En1-lacZ* (pink). Note, that the Wnt7a and *En1/Wnt7a* mutant AERs are slightly wider than the wild-type AER, but much narrower than the *En1* mutant AER. Whole-mount dorsal view (E-G) and high power ventral view (H-J) of young adult wild-type (E,H), *En1* mutant (I), *Wnt7a* mutant (F) and *En1/Wnt7a* double-mutant (G,J) paws. The dorsal surface of a wild-type paw is covered with hair, but lacks dermal pads (E). In contrast, the dorsal surface of *Wnt7a* and *En1/Wnt7a* double-mutant paws (F,G) show variable loss of hair follicles distally and develop ectopic pigmented pads, which grow hard, nail-like structures (arrowheads). In contrast to the ectopic dorsal pads, wild-type ventral pads (H) are soft, compressible bulges with a non-shiny epidermal surface which lacks pigmentation except at the opening of sweat gland ducts. The ventral pads as well as the transverse digit ridges of *En1* mutant (I) and *En1/Wnt7a* (J) double-mutant paws, however, are firm, shiny bulges with marked pigmentation throughout the surface ectoderm. As described previously (Loomis et al., 1997) these go on to form nail-like structures in older mice similar to the ectopic dorsal pads described above. Bar: 500 μm.

The embryonic and postnatal D-V patterning defects in the *En1/Wnt7a* double mutants reflect a combination of the two single mutant D-V phenotypes. As in stage 5/6 *Wnt7a* mutant limbs (Fig. I), the distodorsal expression of *Lmx1b* is lost in *En1/Wnt7a* double-mutant limbs (data not shown). However, the ectopic ventral expression of *Lmx1b* seen in stage 5/6 *En1* mutant limbs was not observed in *En1/Wnt7a* double mutants (data not shown), confirming the dependence of late ventral *Lmx1b* expression on Wnt7a signalling from adjacent ectoderm.

Postnatally, the proximal paws combined the phenotypic characteristics of both the *Wnt7a* and *En1* single mutants, whereas the digit tips resembled those of the *Wnt7a* mutants. The nails of the double mutants, like those of the *Wnt7a* mutants, were shortened cones which were overgrown by

exuberant pad tissue on both dorsal and ventral sides. As in the *Wnt7a* mutants, hair follicles were variably lost from the dorsal digit surfaces and foot pads, which are usually restricted to the ventral paw, developed dorsally on the *En1/Wnt7a* double-mutant paws (Fig. 5E-G). The ectopic dorsal pads in *Wnt7a* and *En1/Wnt7a* double mutants were distinct from wild-type ventral pads in that the dorsal pads were aberrantly pigmented, displayed a paucity of eccrine glands and developed into hard nail-like structures over time. The *En1/Wnt7a* double mutants also developed abnormal ventral pads similar to those observed in *En1* mutant limbs (Fig. 5H-J). These pads, like the aberrant dorsal pads, were highly pigmented and developed hard nail-like surfaces over the first several weeks of life. The two compound heterozygous-homozygous limb phenotypes were indistinguishable from the respective homozygous phenotypes. This analysis demonstrates that *Wnt7a* is required for ectopic AER formation, as well as promoting dorsalization of the limb mesenchyme in *En1* mutants. Independently of *Wnt7a*, *En1* appears to be required for eccrine gland formation and suppression of nail-like structures in association with dermal pads during postnatal development.

DISCUSSION

Detailed analysis of D-V patterning and AER formation in wild-type and *En1* and *Wnt7a* mutant limbs has provided further insights into the genetic and cellular pathways important in these processes. First, our results reinforce previous histological studies suggesting that mouse AER development occurs in multiple stages. Expression of early AER marker genes was found to be induced in a broad region of ectoderm covering the ventral limb and then to become restricted to the tip, and this change in the expression domain appears to coincide with compaction of the ventral ectoderm to form a morphologically visible ridge. Second, we have observed that, in mouse, unlike that reported for chick (Riddle et al., 1995; Vogel et al., 1995), the dorsalizing gene *Lmx1b* is initially expressed in both dorsal and ventral limb mesenchyme and then becomes dorsally restricted just prior to AER formation. In *Wnt7a* mutants, we observed that this early expression of *Lmx1b* is independent of *Wnt7a*. Third, our mutant analysis indicates that *En1* is required during AER formation specifically for maturation of the ventral AER, where it is normally expressed. In *En1* mutants, the dorsal AER appears to form normally, whereas the ventral AER does not compact resulting in an abnormally broadened AER in the ventroproximal dimension. The resulting expanded AER later bifurcates and, in some cases, forms ectopic AERs that can promote digit formation ventrally. Finally, our analysis of *Wnt7a/En1* double-mutant limb buds demonstrates that *Wnt7a* is required for formation of ectopic AERs in *En1* mutants. We suggest that this is because ectopic ventral *Wnt7a* and/or *Lmx1b* expression in *En1* mutants induces ventral AER cells to take on dorsal characteristics and undergo a second compaction process ventrally.

Role of ectodermal morphogenetic movements in early AER formation

The data to date do not distinguish between whether the initial induction of the AER is coincident with formation of a morphologically thickened ridge or begins at an earlier stage. Milaire (1974) proposed that many of the important morphogenetic functions of the definitive AER are present in the ventral ectoderm of the pre-AER limb bud, based on histochemical and morphological studies of early limb buds. He suggested that mammalian AER development involves progressive thickening of the ventral ectoderm and then a convergence of these cells to the limb margin. Consistent with this, recent chick-quail chimera studies and cell-labelling experiments in chick indicate that a lineage relationship exists between cells that initially overlie a broad region of presumptive limb mesoderm and cells that later reside along the ventrodistal surface of the pre-AER limb bud and finally localize to the mature AER (Altabef et al., 1997; Michaud et al., 1997).

Our gene expression studies and morphological data provide further evidence that early morphogenetic movements are critical for normal mouse AER development (Fig. 6A). We showed that, prior to formation of a morphologically distinct AER, the AER marker genes *Dlx2* and *Fgf8* are expressed in a broad region of ventral ectoderm, consistent with prior observations (Lyons et al., 1990; Bulfone et al., 1993; Parr et al., 1993; Crossley and Martin, 1995; Morasso et al., 1995). We went on to further show that the ventro-proximal border of this expression domain shifts distally with increasing limb maturity and that this shift correlates temporally and spatially with the progressive morphological thickening of the ventrodistal limb ectoderm observed by Milaire (1974) (also see Fig. 1). Additionally, the *En1* expression domain initially occupies only the proximal region of the early ventral limb but later extends to the distal margin. It is not clear from our studies if all the *Dlx2/Fgf8*-expressing cells in the ventral ectoderm of the pre-AER limb bud ultimately come to reside in the definitive AER. Indeed, recent cell-labelling studies in chick suggest that this might not be the case (Altabef et al., 1997). Nevertheless the cumulative molecular and morphological data indicate that multiple waves of ectodermal morphogenetic movements are probably critical for normal mouse AER development (Fig. 6A).

Wnt7a and *En1* are required only for late regulation of *Lmx1b*

D-V patterning in the early limb involves complex interactions between mesoderm and ectoderm. Tissue rotation experiments in chick suggested that D-V polarity of the early limb field is initially specified by mesoderm and, just prior to limb outgrowth, control is transferred to the overlying ectoderm (Geduspan and MacCabe, 1989). Given these results, we were somewhat surprised to find that expression of the dorsalizing gene *Lmx1b* is not restricted to early dorsal limb mesenchyme, but expression extends into the ventral mesenchyme. However, by stage 2, *Lmx1b* expression has receded from the ventral mesenchyme, resulting in distinct dorsal and ventral molecular identities of the limb mesoderm.

Analysis of *En1* and *Wnt7a* mutants demonstrated that late, but not early, *Lmx1b* regulation in mouse is dependent on *En1* and *Wnt7a*. In pre-AER *En1* mutant limbs, the lack of *En1* expression and persistent *Wnt7a* expression ventrally has little apparent effect on initiation of *Lmx1b* expression and its subsequent dorsal restriction. However, ventral reexpression of *Lmx1b* does occur in *En1* mutants, at stages 5-6, and this is

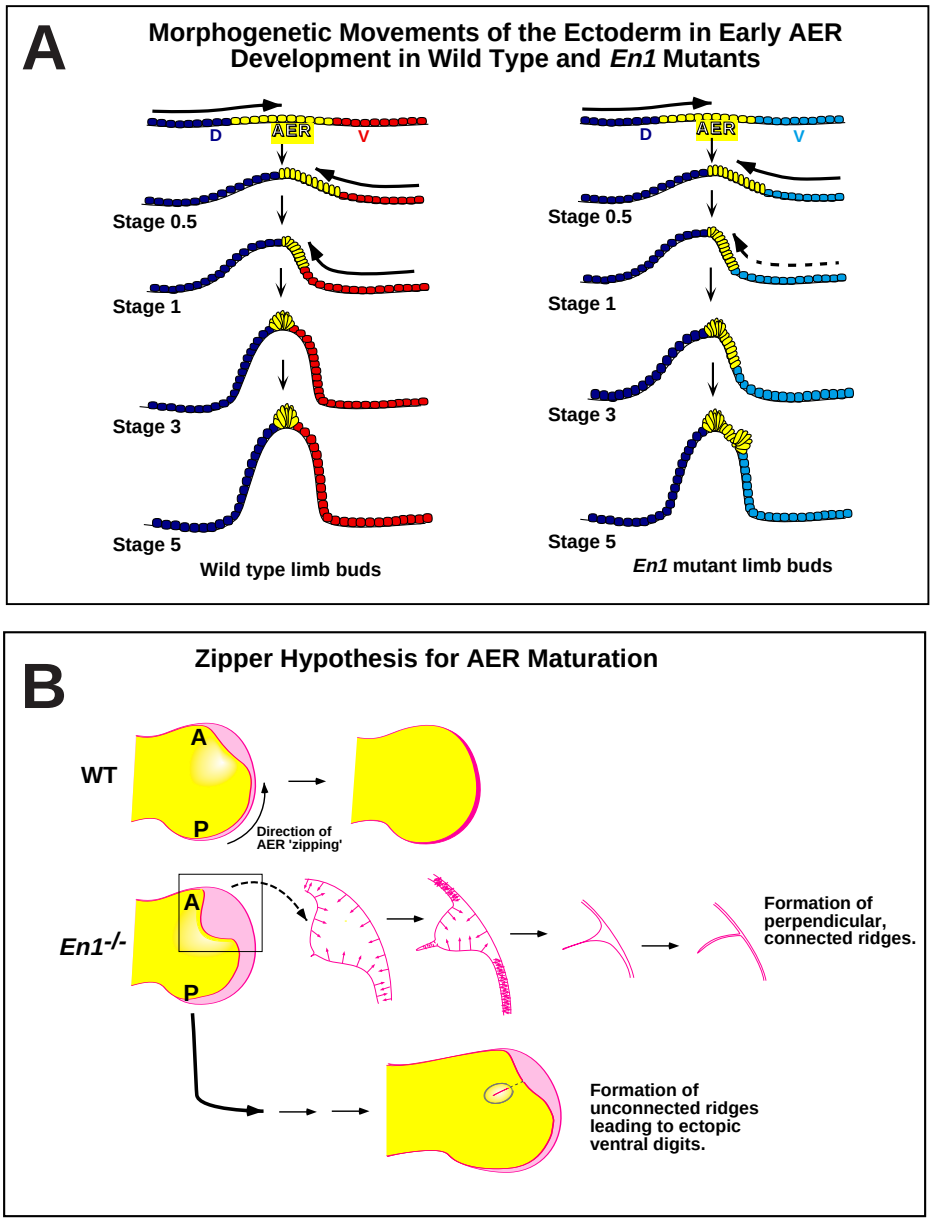

Fig. 6. Schematic drawing illustrating a model for the morphogenetic movements important in mouse AER development. Based on our results, prior histochemical studies in mouse and lineage data in chick (Milaire,1974; Michaud et al., 1997; Altabef et al., 1997), we propose that cells which give rise to the mouse AER initially overlie much of the presumptive limb mesoderm and that sequential, convergent morphogenetic movements are required for normal ridge formation (A, left). A first wave of lateral morphogenetic movements results in the compaction of the AER precursor cells onto the ventral surface of the early limb bud and early ventral ectodermal thickening. A second wave compresses this domain to the distal 1/3 of the ventral limb, and a final wave constricts the cells into the densely packed AER. In *En1* mutants (A, right), the first morphogenetic waves occur normally. The final wave, however, is markedly inhibited and a secondary compaction process is initiated at the ventroproximal border of the widened mutant AER (A, bottom right). We further suggest that this final wave of ectodermal movements resembles the closing of a zipper (B, ventral view of limb). This process initiates posteriorly and proceeds anteriorly, bringing the ventral domain of the wild-type AER into close proximity to the dorsal domain, which is anchored at the D-V interface (top). In *En1* mutant limbs (middle and bottom), the anatomically ventral AER cells take on dorsal characteristics, causing them to become partially anchored and to recruit cells into an ectopic proximoventral rim. The two rims of the bifurcated mutant AER ultimately converge, although in some cases the ventral rim also begins to zip up on itself (middle). If this self-zipping begins at late stages of limb development, the ectopic secondary AER remains contiguous with the primary AER and intersects the latter at a 90° angle (middle, far right); if it begins earlier, the ectopic secondary AER becomes discontinuous with the primary AER and goes on to promote the outgrowth of distinct ventral digits (bottom).

dependent on *Wnt7a* expression as it does not occur in *En1/Wnt7a* double mutants. Furthermore, in *Wnt7a* mutant limbs, *Lmx1b* expression is normal until stages 5-6, when it is lost dorsally, but only in distal regions, consistent with a study in chick demonstrating selective distal loss of *Lmx1b* expression after removal of the *Wnt7a* expressing dorsal ectoderm (Riddle et al., 1995).

Loss of *En1* leads to aberrant ventral AER maturation and the formation of ectopic AERs

Our mutant studies have demonstrated that *En1* is not required for the process of AER induction or the initial stages of AER formation. Loss of *En1* function has no apparent effect on the early thickening of the pre-AER ventral ectoderm (stage 0.5-1) or on the initial induction of AER marker genes, such as *Dlx2* and *Fgf8*. Furthermore, at stage 3, the cells of the dorsal AER of *En1* mutant limbs, like those of wild-type limbs, do not express *Wnt7a* and they stratify and initiate *Fgf4* expression, an AER differentiation marker (Niswander et al., 1994; Chan et al., 1995; Haramis et al., 1995).

In contrast, differentiation of the ventral portion of the AER, where *En1* is normally expressed, appears to be delayed and abnormal in *En1* mutants. At the time when a mature AER is apparent in wild-type limbs, the ventral portion of the *En1* mutant AER remains extended with the anterior region being much broader than the posterior. This difference in the *En1* mutant AER phenotype along the A-P axis likely reflects an exaggeration of the inherent A-P asymmetry characteristic of

normal ridge constriction, which begins posteriorly and proceeds anteriorly (see Fig. 2G; Milaire, 1974). The ventral AER cells of stage 3/4 *En1* mutants remain relatively flat and, while they express *Dlx2* and *Fgf8*, they do not express *Fgf4* (Fig. 2L) and do not repress expression of *Wnt7a* until late (Loomis et al., 1996 and Fig. 2B,F). Nevertheless, the ventral AERs of *En1* mutants appear to have some characteristics of a functional AER, since the underlying mesenchyme proliferates. In fact, the expanded *En1* mutant ventral AER at these stages appears to secrete more growth factors than normal, since the anterior ventrodistal mesenchyme is visibly wider than normal and it expresses genes usually restricted to AER-associated distal mesenchyme, such as *Msx2* (data not shown).

Roughly coincident with the up-regulation of the dorsalizing gene *Lmx1b* in the ventral mesenchyme of stage 5/6 *En1* mutant limbs, the cells along the ventral border of the expanded AER begin to thicken (Fig. 6A) and occasionally initiate *Fgf4* expression. Morphologically, the AER of *En1* mutants appears bifurcated with the two rims being markedly further apart anteriorly than posteriorly. In some cases (~30%), independent ectopic AERs form, which display prolonged expression of AER marker genes and go on to promote either independent digit outgrowths or partial distal digit duplications on the ventral surface of *En1* mutants limbs.

Based on these observations, we propose a model that likens the final phase of AER constriction to the closing of a zipper (Fig. 6B). In wild-type limb buds, the two halves of the zipper are the dorsal and ventral AER domains. The zipping occurs between stages 1 and 3 with the dorsal half remaining relatively fixed and the ventral half being pulled towards it in a posterior-to-anterior direction. In *En1* mutants, differentiation of the ventral half of the AER is markedly delayed and the cells eventually acquire characteristics of dorsal AER cells. Although a zipping process occurs in the normal posterior-to-anterior direction in *En1* mutants, the cells in the middle of the broadened AER are pulled toward both the dorsal and ventral AER borders due to the transformation of the ventral half of the AER into a functionally 'dorsal' AER. In some cases, distinct secondary AERs form, at right angles to the normal AER axis, due to self-zipping of the ectopic rim (Figs 2B, 4D-H, 6B).

Role of *Wnt7a* in ectopic AER formation in *En1* mutants

The finding that, in *En1/Wnt7a* double mutants, bifurcated AERs do not form, nor do later ectopic AERs or ventral digits, demonstrates that *Wnt7a* is required for initiation of abnormal secondary AER formation in *En1* mutants. In addition, the finding supports our suggestion that the early abnormal AER structures seen in *En1* mutants later produce ectopic ventral digits. Since the AER of *En1/Wnt7a* double mutants is only slightly broader than normal, this indicates that the early ventral expression of *Wnt7a* in *En1* mutants plays a role in the delay in compaction of the ventral AER cells. This could be due to early expression of *Wnt7a* in the ventral AER; for example, if *Wnt7a* prevents necessary cell-shape changes. Alternatively, if during normal limb development *Wnt7a* secreted from the dorsal non-AER ectoderm is involved in specifying the adjacent AER cells to take on a dorsal phenotype then, in *En1* mutants, the ectopic signalling of *Wnt7a* ventrally would lead to specification of the ventral AER cells as dorsal. Since one apparent characteristic of dorsal AER cells is to stay anchored and pull or recruit cells toward them, this could account for the initial delay in compaction of the *En1* mutant ventral AER cells and the later formation of a bifurcated AER.

With respect to the question of the genetic mechanism by which *Wnt7a* expression leads to formation of secondary AERs in *En1* mutants, it is interesting to note that the position of the secondary AER thickening roughly coincides with both the timing of, and the contour of, the ectopic ventral *Lmx1b* expression domain. Furthermore, in the *En1* mutants, ectopic ventral digits and AERs never develop in the posterior autopod where ventral *Lmx1b* expression is not maintained (Fig. 4J). Since in *En1/Wnt7a* double mutants *Lmx1b* is not reexpressed in the ventral mesenchyme, it is possible that *Lmx1b* also plays a role in the stratification of the ventroproximal AER border and formation of a bifurcated AER.

In *Wnt7a* mutants, the dorsal AER is only slightly broader than normal, indicating that *Wnt7a* alone does not normally play a major role in AER formation. Since, *Lmx1b* is expressed in the dorsal mesenchyme of *Wnt7a* mutant limbs at the time of AER formation, it is possible that *Lmx1b* might compensate for the lack of *Wnt7a* expression in the dorsal ectoderm. Alternatively, or in addition, another *Wnt* gene might partially compensate for loss of *Wnt7a* dorsally. It will be interesting to determine whether the Notch pathway also regulates the later process of AER maturation and/or earlier process of AER induction.

In summary, *En1* is essential for the normal maturation of the ventral AER, as well as ventral limb patterning. The proper compaction and stratification to form a mature AER requires *En1*. Our studies indicate that the process of forming ectopic AERs in *En1* mutants does not involve a recapitulation of the entire process of AER formation, but instead involves duplication of part of the later process of AER differentiation. We suggest that this formation of a second dorsal AER domain and focal ectodermal thickening requires the juxtaposition of presumptive AER ectoderm and functionally dorsal non-AER ectoderm or mesoderm. These studies have provided a unique example of a genetic pathway impacting on both cell fate and morphogenetic movements, which combine to generate form and pattern.

We thank E. Harris for excellent technical help; Sheila Bell and Bill Scott for provocative discussions; R. Johnson, G. Martin, C. Mahon and M. Morasso for sharing plasmids; Andy McMahon and J. Cygan for sharing mice, plasmids and advice; D-L Song and C. Breigel for help developing a PCR assay for *En1* mutants; and C. Breigel for comments and review of the manuscript. A. L. J. is a Howard Hughes Investigator and C. A. L. has been supported by a Dermatology Foundation Career Development Award and an NIH Training Grant number ARO7190T32A7190.

REFERENCES

Akita, K. (1996). The effect of the ectoderm on the dorsoventral pattern of epidermis, muscles and joints in the developing chick leg: a new model. *Anatomy & Embryology* **193**, 377-386.

Altabef, M., Clarke, J. D. W. and Tickle, C. (1997). Dorso-ventral ectodermal compartments and origin of apical ectodermal ridge in developing chick limb. *Development* **124**, 4547-4556.

Bulfone, A., Kim, H. J., Puelles, L., Porteus, M. H., Grippo, J. F. and

Rubenstein, J. L. (1993). The mouse Dlx-2 (Tes-1) gene is expressed in spatially restricted domains of the forebrain, face and limbs in midgestation mouse embryos. *Mech. Dev.* **40**, 129-140.

Chan, D. C., Laufer, E., Tabin, C. and Leder, P. (1995). Polydactylous limbs in Strong's Luxoid mice result from ectopic polarizing activity. *Development* **121**, 1971-1978.

Crossley, P. H. and Martin, G. R. (1995). The mouse Fgf8 gene encodes a family of polypeptides and is expressed in regions that direct outgrowth and patterning in the developing embryo. *Development* **121**, 439-451.

Crossley, P. H., Minowada, G., MacArthur, C. A. and Martin, G. R. (1996). Roles for FGF8 in the induction, initiation, and maintenance of chick limb development. *Cell* **84**, 127-136.

Cygan, J. A., Johnson, R. L. and McMahon, A. P. (1997). Novel regulatory interactions revealed by studies of murine limb pattern in Wnt-7a and En-1 mutants. *Development* **124**, 5021-5032.

Davis, C. A., Holmyard, D. P., Millen, K. J. and Joyner, A. L. (1991). Examining pattern formation in mouse, chicken and frog embryos with an En-specific antiserum. *Development* **111**, 287-298.

Gardner, C. A. and Barald, K. F. (1992). Expression patterns of engrailed-like proteins in the chick embryo. *Dev. Dynamics* **193**, 370-388.

Geduspan, J. S. and MacCabe, J. A. (1987). The ectodermal control of mesodermal patterns of differentiation in the developing chick wing. *Dev. Biol.* **124**, 398-408.

Geduspan, J. S. and MacCabe, J. A. (1989). Transfer of dorsoventral information from mesoderm to ectoderm at the onset of limb development. *Anatomical Record* **224**, 79-87.

Grieshammer, U., Minowada, G., Pisenti, J. M., Abbott, U. K. and Martin, G. R. (1996). The chick limbless mutation causes abnormalities in limb bud dorsal-ventral patterning: implications for the mechanism of apical ridge formation. *Development* **122**, 3851-3861.

Hanks, M., Wurst, W., Anson-Cartwright, L., Auerbach, A. B. and Joyner, A. L. (1995). Rescue of the En-1 mutant phenotype by replacement of En-1 with En-2 [see comments]. *Science* **269**, 679-682.

Haramis, A. G., Brown, J. M. and Zeller, R. (1995). The limb deformity mutation disrupts the SHH/FGF-4 feedback loop and regulation of 5′ HoxD genes during limb pattern formation. *Development* **121**, 4237-4245.

Johnson, R. L., Riddle, R. D. and Tabin, C. J. (1994). Mechanisms of limb patterning. *Curr. Opin. Genet. Dev.* **4**, 535-542.

Jurand, A. (1965). Ultrastructural aspects of early development of the fore-limb buds in the chick and the mouse. *Proc. Royal Soc.* **162**, 387-405.

Kelley, R. O. and Fallon, J. F. (1983). A freeze-fracture and morphometric analysis of gap junctions of limb bud cells: initial studies on a possible mechanism for morphogenetic signalling during development. *Progress in Clinical & Biological Research* **110**, 119-130.

Laufer, E., Dahn, R., Orozco, O. E., Yeo, C. Y., Pisenti, J., Henrique, D., Abbott, U. K., Fallon, J. F. and Tabin, C. (1997). Expression of Radical fringe in limb-bud ectoderm regulates apical ectodermal ridge formation [see comments]. *Nature* **386**, 366-373.

Laufer, E., Nelson, C. E., Johnson, R. L., Morgan, B. A. and Tabin, C. (1994). Sonic hedgehog and Fgf-4 act through a signaling cascade and feedback loop to integrate growth and patterning of the developing limb bud. *Cell* **79**, 993-1003.

Lindsell, C. E., Shawber, C. J., Boulter, J. and Weinmaster, G. (1995). Jagged: a mammalian ligand that activates Notch1. *Cell* **80**, 909-917.

Logan, C., Hornbruch, A., Campbell, I. and Lumsden, A. (1997). The role of Engrailed in establishing the dorsoventral axis of the chick limb. *Development* **124**, 2317-2324.

Loomis, C. A., Harris, E., Michaud, J., Wurst, W., Hanks, M. and Joyner, A. L. (1996). The mouse Engrailed-1 gene and ventral limb patterning. *Nature* **382**, 360-363.

Lyons, K. M., Pelton, R. W. and Hogan, B. L. (1990). Organogenesis and pattern formation in the mouse: RNA distribution patterns suggest a role for bone morphogenetic protein-2A (BMP-2A). *Development* **109**, 833-844.

MacCabe, J. A., Errick, J. and Saunders, J. W., Jr. (1974). Ectodermal control of the dorsoventral axis in the leg bud of the chick embryo. *Dev. Biol.* **39**, 69-82.

Mahmood, R., et al. (1995). A role for FGF-8 in the initiation and maintenance of vertebrate limb bud outgrowth. *Current Biology* **5**, 797-806.

Martin, G. R. (1995). Why thumbs are up. *Nature* **374**, 410-411.

Matise, M. P. and Joyner, A. L. (1997). Expression patterns of developmental control genes in normal and Engrailed-1 mutant mouse spinal cord reveal early diversity in developing interneurons. *J. Neurosci.* **17**, 7805-7816.

Meinhardt, H. (1983). Cell determination boundaries as organizing regions for secondary embryonic fields. *Dev. Biol.* **96**, 375-385.

Michaud, J. L., Lapointe, F. and Le Douarin, N. M. (1997). The dorsoventral polarity of the presumptive limb is determined by signals produced by the somites and by the lateral somatopleure. *Development* **124**, 1453-1463.

Milaire, J. (1974). Histochemical aspects of organogenesis in vertrebrates. Part I. The skeletal system. Limb morphogenesis. The sense organs. In *Handbuch der Histochemie* pp. 38-60., Stuttgart: Gustav Fischer Verlag.

Morasso, M. I., Mahon, K. A. and Sargent, T. D. (1995). A Xenopus distal-less gene in transgenic mice: conserved regulation in distal limb epidermis and other sites of epithelial-mesenchymal interaction. *Proc. Natl. Acad. Sci. USA* **92**, 3968-3972.

Niswander, L. (1996). Growth factor interactions in limb development. *Ann. N.Y. Acad. Sci.* **785**, 23-26.

Niswander, L., Jeffrey, S., Martin, G. R. and Tickle, C. (1994). A positive feedback loop coordinates growth and patterning in the vertebrate limb [see comments]. *Nature* **371**, 609-612.

Niswander, L. and Martin, G. R. (1992). Fgf-4 expression during gastrulation, myogenesis, limb and tooth development in the mouse. *Development* **114**, 755-768.

Niswander, L. and Martin, G. R. (1993). FGF-4 regulates expression of Evx-1 in the developing mouse limb. *Development* **119**, 287-294.

Niswander, L., Tickle, C., Vogel, A., Booth, I. and Martin, G. R. (1993). FGF-4 replaces the apical ectodermal ridge and directs outgrowth and patterning of the limb. *Cell* **75**, 579-587.

Niswander, L., Tickle, C., Vogel, A. and Martin, G. (1994). Function of FGF-4 in limb development. [Review]. *Mol. Reprod. Dev.* **39**, 83-88.

Noramly, S., Pisenti, J., Abbott, U. and Morgan, B. (1996). Gene expression in the limbless mutant: polarized gene expression in the absence of Shh and an AER. *Dev. Biol.* **179**, 339-346.

Ohuchi, H., Shibusawa, M., Nakagawa, T., Ohata, T., Yoshioka, H., Hirai, Y., Nohno, T., Noji, S. and Kondo, N. (1997). A chick wingless mutation causes abnormality in maintenance of Fgf8 expression in the wing apical ridge, resulting in loss of the dorsoventral boundary. *Mech. Dev.* **62**, 3-13.

Ohuchi, H., Yoshioka, H., Tanaka, A., Kawakami, Y., Nohno, T. and Noji, S. (1994). Involvement of androgen-induced growth factor (FGF-8) gene in mouse embryogenesis and morphogenesis. *Biochem. Biophys. Res. Comm.* **204**, 882-888.

Parr, B. A. and McMahon, A. P. (1995). Dorsalizing signal Wnt-7a required for normal polarity of D-V and A-P axes of mouse limb. *Nature* **374**, 350-353.

Parr, B. A., Shea, M. J., Vassileva, G. and McMahon, A. P. (1993). Mouse Wnt genes exhibit discrete domains of expression in the early embryonic CNS and limb buds. *Development* **119**, 247-261.

Pautau, M. P. (1977). *Vertebrate Limb and Somite Morphogenesis* (ed. Ede, D. A., Hinchliffe, J. R. and Balls, M.) Cambridge: Cambridge University Press.

Pautou, M. P. and Kieny, M. (1973). Interaction ec-mesodermique dans l'establissement de la polarite dorso-ventrale du pied de l'embryon de poulet. *C.r. hebd Seanc. Acad. Sci., Paris* **D277**.

Prahlad, K. V., Skala, G., Jones, D. G. and Briles, W. E. (1979). Limbless: a new genetic mutant in the chick. *J. Exp. Zool.* **209**, 427-434.

Riddle, R. D., Ensini, M., Nelson, C., Tsuchida, T., Jessell, T. M. and Tabin, C. (1995). Induction of the LIM homeobox gene Lmx1 by WNT7a establishes dorsoventral pattern in the vertebrate limb. *Cell* **83**, 631-640.

Riddle, R. D., Johnson, R. L., Laufer, E. and Tabin, C. (1993). Sonic hedgehog mediates the polarizing activity of the ZPA. *Cell* **75**, 1401-1416.

Robinson, G. W. and Mahon, K. A. (1994). Differential and overlapping expression domains of Dlx-2 and Dlx-3 suggest distinct roles for Distal-less homeobox genes in craniofacial development. *Mech. Dev.* **48**, 199-215.

Rodriguez-Esteban, C., Schwabe, J. W., De La Pena, J., Foys, B., Eshelman, B. and Belmonte, J. C. (1997). Radical fringe positions the apical ectodermal ridge at the dorsoventral boundary of the vertebrate limb [see comments]. *Nature* **386**, 360-366.

Ros, M. A., Lopez-Martinez, A., Simandl, B. K., Rodriguez, C., Izpisua Belmonte, J. C., Dahn, R. and Fallon, J. F. (1996). The limb field mesoderm determines initial limb bud anteroposterior asymmetry and budding independent of sonic hedgehog or apical ectodermal gene expressions. *Development* **122**, 2319-2330.

Saunders, J. W., Jr. (1948). The proximo-distal sequence of the origin of the parts of the chick wing and the role of th ectoderm. *J. Exp. Zool.* **108**, 363-404.

Saunders, J. W., Jr. and Gasseling, M. T. (1968). *Epithelial-Mesenchymal*

Interactions (ed. Fleischmajer, R. and Billingham, R. E.) Baltimore: Williams and Wilkins.

Sidow, A., et al. (1997). Serrate2 is disrupted in the mouse limb-development mutant syndactylism. *Nature* **389**, 722-725.

Tanaka, M., Tamura, K., Noji, S., Nohno, T. and Ide, H. (1997). Induction of additional limb at the dorsal-ventral boundary of a chick embryo. *Dev. Biol.* **182**, 191-203.

Tickle, C. (1995). Vertebrate limb development. *Curr. Opin. Genet. Dev.* **5**, 478-484.

Vogel, A., Rodriguez, C. and Izpisua-Belmonte, J. C. (1996). Involvement of FGF-8 in initiation, outgrowth and patterning of the vertebrate limb. *Development* **122**, 1737-1750.

Vogel, A., Rodriguez, C., Warnken, W. and Izpisua Belmonte, J. C. (1995). Dorsal cell fate specified by chick Lmx1 during vertebrate limb development. *Nature* **378**, 716-720.

Wanek, N., Muneoka, K., Holler-Dinsmore, G., Burton, R. and Bryant, S. V. (1989). A staging system for mouse limb development. *J. Exp. Zool.* **249**, 41-49.

Wurst, W., Auerbach, A. B. and Joyner, A. L. (1994). Multiple developmental defects in Engrailed-1 mutant mice: an early mid-hindbrain deletion and patterning defects in forelimbs and sternum. *Development* **120**, 2065-2075.

Yang, Y. and Niswander, L. (1995). Interaction between the signaling molecules WNT7a and SHH during vertebrate limb development: dorsal signals regulate anteroposterior patterning. *Cell* **80**, 939-947.

Zeller, R. and Duboule, D. (1997). Dorso-ventral limb polarity and origin of the ridge: on the fringe of independence? *BioEssays* **19**, 541-546.